

Thermal properties and crystallization kinetics of tellurium oxide based glasses

E.D. Jeong^a, J.S. Bae^a, T.E. Hong^a, K.T. Lee^b, B.K. Ryu^b, T. Komatsu^c and H.G. Kim^{a,*}

^aBusan Center, Korea Basic Science Institute, Busan 609-735, Korea

^bSchool of Materials Science & Technology, Pusan National University, Busan 609-735, Korea

^cDepartment of Chemistry, Nagaoka University of Technology, Nagaoka 940-21, Japan

The thermal stabilities and formation kinetics of $K[Nb_{1/3}Te_{2/3}]_2O_{4.8}$ phase in $K_2O-Nb_2O_5-TeO_2$ glasses were investigated. The activation energies for crystallization and grain growth of the $K[Nb_{1/3}Te_{2/3}]_2O_{4.8}$ phase from original glasses were determined from the results of XRD and DTA data. Transparent $15K_2O-15Nb_2O_5-70TeO_2$ glass-ceramics have a cubic structure basically, but the cubic structure is very slightly distorted. The activation energy for grain growth of the $K[Nb_{1/3}Te_{2/3}]_2O_{4.8}$ phase in $15K_2O-15Nb_2O_5-70TeO_2$ glass was 33.5 kJ/mol. The energy required for the phase transformation from $15K_2O-15Nb_2O_5-70TeO_2$ glass to $K[Nb_{1/3}Te_{2/3}]_2O_{4.8}$ was 253.6 kJ/mol. The study on the formation kinetics of transparent glass-ceramics with SHG should have a large impact for the development of nonlinear optical materials.

Key words: Activation energy, Thermal stability, Phase transformation, Nano-crystal

Introduction

Tellurium oxide (TeO_2)-based glasses are of scientific and technical interest on account of their low melting temperatures, high refractive indices, high dielectric constants and good infrared transmissions, and thus recently have been considered as promising materials for use in optical fibers or nonlinear optical devices [1-6]. Furthermore, the structure of TeO_2 -based glasses is of interest, because there are two types of basic structural unit, i.e. a TeO_4 trigonal bipyramid with a lone pair electron in an equatorial position and a TeO_3 trigonal bipyramid [7, 8]. Tanaka et al. [9] observed second harmonic generation (SHG) in electrically poled $Li_2O-Nb_2O_5-TeO_2$ and $Nb_2O_5-TeO_2$ glasses. Kim and Yoko [10] measured the third-order nonlinear optical susceptibilities, $\lambda^{(3)}$, of various TeO_2 -based glasses containing transition metal oxides and reported that $30Nb_2O_5-70TeO_2$ glass shows a very large value of $\lambda^{(3)}$. Recently, the present authors' group [11-13] succeeded in fabricating transparent glass-ceramics from the system $K_2O-Nb_2O_5-TeO_2$ and discovered that the crystallized glasses show a second harmonic generation (SHG). Further, in optically transparent Er^{3+} -doped tellurite glass-ceramic, it was found that the intensity of the frequency up-conversion fluorescence at around 550 nm is strong compared with that in their precursor glass [14]. It was also demonstrated that the Vickers hardness of transparent tellurite glass ceramics is much larger than that

of the precursor glass, meaning an improvement in the poor mechanical properties of tellurite glasses [15]. These previous studies indicate that not only TeO_2 -based glasses but also their glass-ceramics have a high potential as new optically functional materials. In previous papers [11-13], it has been proposed that the chemical composition of the crystalline phase showing SHG in the $K_2O-Nb_2O_5-TeO_2$ glass-ceramics is close to $K[Nb_{1/3}Te_{2/3}]_2O_{4.8}$ having an oxygen-defect fluorite structure [14, 15]. The cubic crystalline phase is isotropic and has an inversion symmetry from a macroscopic standpoint which does not allow second-order nonlinear optical processes. A slight distortion from the cubic structure in the crystalline phase formed in TeO_2 -based glass-ceramics had been proposed, which leads to the SHG.

Although $K_2O-Nb_2O_5-TeO_2$ glass-ceramics have been widely studied for the second-order nonlinear optical phenomenon and structure [16-18], the crystallization of the $K[Nb_{1/3}Te_{2/3}]_2O_{4.8}$ phase from precursor samples has not been investigated. In the present study, the formation kinetics and crystallization behavior of $K[Nb_{1/3}Te_{2/3}]_2O_{4.8}$ in $K_2O-Nb_2O_5-TeO_2$ glasses were investigated using X-ray diffraction (XRD) and differential thermal analysis (DTA). The activation energies for crystallization of $K[Nb_{1/3}Te_{2/3}]_2O_{4.8}$ were obtained from these data.

Experimental

Glasses in the series $K_2O-Nb_2O_5-TeO_2$ were prepared using a conventional melt-quenching method. Commercial powders of reagent grade K_2CO_3 (99.5%, Nacal tesque), Nb_2O_5 (99.9%, Soekawa Chemicals) and TeO_2

*Corresponding author:
Tel : +82-51-510-1903
Fax : +82-51-517-2497
E-mail: hhgkim@kbsi.re.kr

(99%, Soekawa Chemicals) were mixed and melted in a platinum crucible at 1000 °C for 40 minutes in an electric furnace. The batch weight was 20g. The liquids were poured onto a carbon plate heated at 250 °C. The glassy state in the quenched samples and the crystalline phase present in the heat-treated samples were characterized by X-ray diffraction (XRD) analysis at room temperature using $\text{CuK}\alpha$ radiation. XRD peaks were compared with data from the Joint Committee Powder Diffraction Standard (JCPDS) for identification of the phases formed. The densities of glasses and heat-treated samples were determined by the Archimedes method using ethanol as the immersion liquid. The refractive indices at a wavelength of 632.8 nm (He-Ne laser) were measured at room temperature using an ellipsometer (Mizojiri Optical Co., DVA-36L model). The glass transition, T_g and crystallization peak, T_x , temperatures were determined using differential thermal analysis (DTA). DTA were carried out at room temperature ranging to 30-1000 °C with various heating rates of 10, 20, 25 and 30 K minute^{-1} .

Results and Discussion

The values of glass the transition temperature, T_g , crystallization onset temperature, T_x , and melting temperature, T_m , for $(30-x)\text{K}_2\text{O}-x\text{Nb}_2\text{O}_5-70\text{TeO}_2$ glasses are given in Table 1. In $(30-x)\text{K}_2\text{O}-x\text{Nb}_2\text{O}_5-70\text{TeO}_2$ glasses both T_g (268-427 °C) and T_x (305-537 °C) increase monotonically with increasing $\text{Nb}_2\text{O}_5/\text{K}_2\text{O}$ ratio. As can be seen in Table 1 it is obvious that the increases in ΔT in $(30-x)\text{K}_2\text{O}-x\text{Nb}_2\text{O}_5-70\text{TeO}_2$ glasses mainly result from the increases in T_x . This implies that the Nb_2O_5 added acts effectively as an inhibitor of crystallization. On the other hand it is reasonable to assume that K_2O , being an alkali oxide, acts mainly as a network breaking agent to decrease T_g and T_m , because both T_g and T_m decrease with increasing K_2O content. Bahgat et al. [19] suggest that in a $15\text{K}_2\text{O}-85\text{TeO}_2$ glass K^+ with a small polarizing power will generate an excess amount of nonbridging oxygens.

Values of density, ρ , and refractive index, n , for the glasses are also given in Table 1. In $(30-x)\text{K}_2\text{O}-x\text{Nb}_2\text{O}_5-70\text{TeO}_2$ glasses both ρ (4.17-4.95 gcm^{-3}) and n (1.85-2.08) increase gradually with increasing $\text{Nb}_2\text{O}_5/\text{TeO}_2$

Table 1. Values of glass transition, T_g , crystallization onset, T_x and melting, T_m , temperatures, density, ρ , and refractive index, n , for $(30-x)\text{K}_2\text{O}-x\text{Nb}_2\text{O}_5-70\text{TeO}_2$ glasses

x	T_g (°C)	T_x (°C)	T_m (°C)	ρ (g/cm^3)	n
5	268	305	465	4.17	1.85
10	328	400	697	4.35	1.92
15	375	491	710	4.46	1.98
17	407	547	664	4.81	2.03
20	427	537	700	4.95	2.08

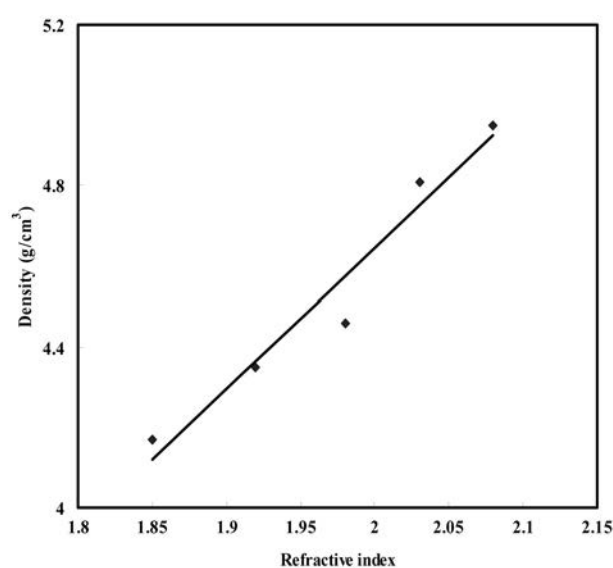


Fig. 1. Correlation between density and refractive index for $(30-x)\text{K}_2\text{O}-x\text{Nb}_2\text{O}_5-70\text{TeO}_2$.

ratio. It is clear that both ρ and n decrease effectively due to the addition of K_2O which is an alkali oxide. The relationship between ρ and n are shown in Figure 1. A good correlation is observed between them indicating that the refractive index increases almost linearly with increasing density. For technical applications it is important to be able to prepare TeO_2 -based glasses with both a high refractive index of over $n=2.0$ and high thermal stability.

Figure 2 shows powder XRD patterns at room temperature for the original glass and heat-treated samples of $15\text{K}_2\text{O}-15\text{Nb}_2\text{O}_5-70\text{TeO}_2$, as a typical example. A crystalline phase appeared in the sample heat-treated at 425 °C

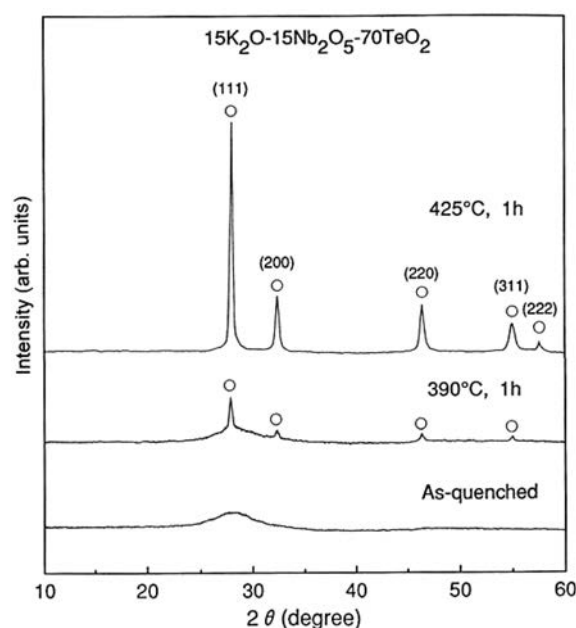


Fig. 2. Powder XRD patterns at room temperature for the original glass and heat-treated samples of $15\text{K}_2\text{O}-15\text{Nb}_2\text{O}_5-70\text{TeO}_2$.

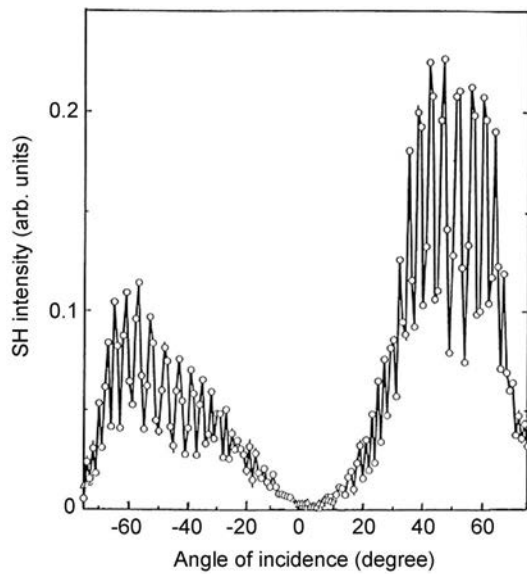


Fig. 3. SHG intensity of transparent 15K₂O-15Nb₂O₅-70TeO₂ glass-ceramics.

°C for 1h is assigned to a face-centered cubic structure with a lattice constant of $a=5.53 \text{ \AA}$. This assignment was also confirmed by using transmission electron microscopy (HITACHI, H-800UHR, 200 kV), which it indicated a cubic structure with $a=5.54 \text{ \AA}$. The chemical composition of the cubic crystalline phase was $\text{K}[\text{Nb}_{1/3}\text{Te}_{2/3}]_2\text{O}_{4.8}$. Transparent 15K₂O-15Nb₂O₅-70TeO₂ glass-ceramics have a cubic structure basically, but the cubic structure is very slightly distorted. SHG was observed in the heat-treated samples consisting of the $\text{K}[\text{Nb}_{1/3}\text{Te}_{2/3}]_2\text{O}_{4.8}$ phase, as shown later, but not in the original glass and the samples heat-treated at temperatures above 450 °C.

Figure 3 shows the variation of SHG with angle of incidence for transparent 15K₂O-15Nb₂O₅-70TeO₂ glass-ceramics consisting of the $\text{K}[\text{Nb}_{1/3}\text{Te}_{2/3}]_2\text{O}_{4.8}$ phase, indicating that a SHG takes place in this glass-ceramic. The maximum SH intensity of transparent 15K₂O-15Nb₂O₅-70TeO₂ glass-ceramics is observed at incident angles of 40°-50°. The SH intensity in this glass-ceramics shown in Figure 3 is comparable to that in electrically poled TeO₂-based glasses [9, 20].

The crystallite size of the $\text{K}[\text{Nb}_{1/3}\text{Te}_{2/3}]_2\text{O}_{4.8}$ phase formed in the 15K₂O-15Nb₂O₅-70TeO₂ glass was estimated from the full width at half maximum intensity (FWHM) of an XRD peak (Fig. 2) using Scherrers equation [21]:

$$L=0.9\lambda/B\cos\theta \quad (1)$$

where λ is the wavelength of the X-ray radiation ($\lambda=0.154 \text{ nm}$), B is the FWHM of the peak (radians) corrected for instrumental broadening, θ is the Bragg angle, and L is the crystallite size (\AA). The crystallite sizes for the $\text{K}[\text{Nb}_{1/3}\text{Te}_{2/3}]_2\text{O}_{4.8}$ phase are given in Table 2. The crystallite size of the $\text{K}[\text{Nb}_{1/3}\text{Te}_{2/3}]_2\text{O}_{4.8}$ phase increased rapidly with increasing heat treatment temper-

Table 2. Crystallite sizes of the $\text{K}[\text{Nb}_{1/3}\text{Te}_{2/3}]_2\text{O}_{4.8}$ formed in 15K₂O-15Nb₂O₅-70TeO₂ samples heat-treated at various temperatures

Temperature (°C)	Crystallite size (nm)
390	7
400	19
410	26
420	30

ature. The activation energy required for grain growth of $\text{K}[\text{Nb}_{1/3}\text{Te}_{2/3}]_2\text{O}_{4.8}$ phase in 15K₂O-15Nb₂O₅-70TeO₂ glass could be estimated by the Arrhenius plot of the results shown in Table 2.

According to Coble's theory [22], the activation energy for grain growth can be calculated from the Arrhenius equation:

$$d \ln k/dT=E/RT^2, \quad (2)$$

where k is the specific reaction rate constant, E is the activation energy, T is the absolute temperature and R is the ideal gas constant.

Jarcho et al. [23] discovered that the value of k was related with the grain size directly. Thus modification and integration Eq. (2) becomes:

$$\log D=(-E/2.303 R)/T+A, \quad (3)$$

where D is the grain size and A is intercept. From a plot of $\log D$ versus the reciprocal of absolute temperature ($1/T$) from Eq. (3), one obtains a straight-line as shown in Figure 4. The slope of this line gives the activation energy for grain growth of the $\text{K}[\text{Nb}_{1/3}\text{Te}_{2/3}]_2\text{O}_{4.8}$ phase in 15K₂O-15Nb₂O₅-70TeO₂ glass. Activation energy of grain growth of $\text{K}[\text{Nb}_{1/3}\text{Te}_{2/3}]_2\text{O}_{4.8}$ phase was determined to be 33.5 kJ/mol.

Thermal behaviors of 15K₂O-15Nb₂O₅-70TeO₂ glass were investigated by DTA. The values of T_g and T_x for

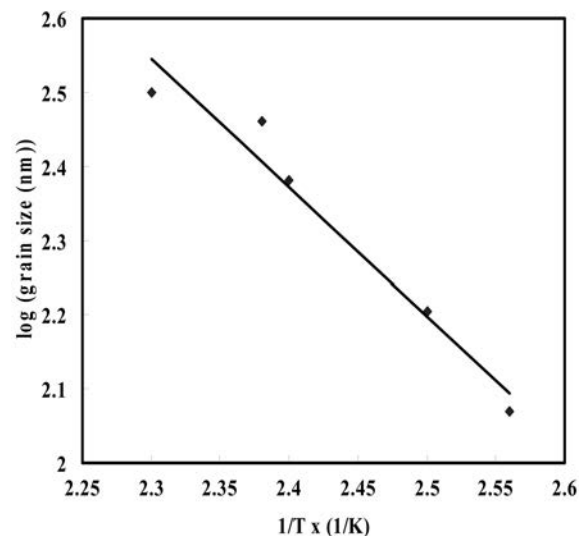


Fig. 4. A plot of \log (grain size of $\text{K}[\text{Nb}_{1/3}\text{Te}_{2/3}]_2\text{O}_{4.8}$ formed in the 15K₂O-15Nb₂O₅-70TeO₂ glass heat-treated at various temperatures) versus the reciprocal of absolute temperature ($1/T$) $\times 1000$.

Table 3. Values of T_g and T_x for $15K_2O-15Nb_2O_5-70TeO_2$ glasses in the temperature range of 50-900°C with different heating rates of 10, 20, 25 and 30 K $minute^{-1}$

Heating rate	T_g (°C)	T_x (°C)
10 K $minute^{-1}$	375.51	491.33
20 K $minute^{-1}$	373.78	502.62
25 K $minute^{-1}$	379.08	505.21
30 K $minute^{-1}$	382.37	508.57

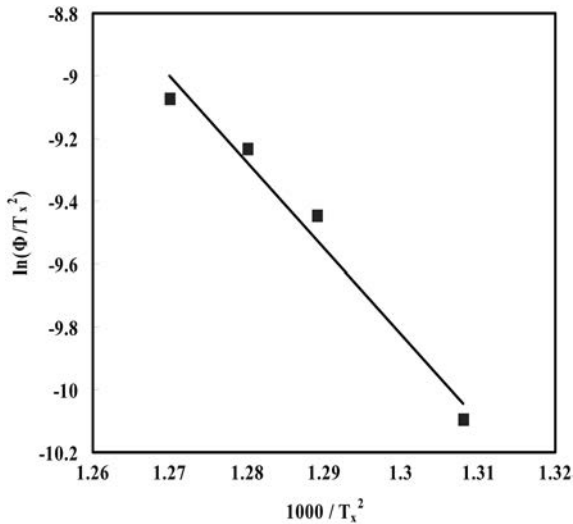


Fig. 5. A plot to obtain the activation energy involved in the amorphous to crystallization $K[Nb_{1/3}Te_{2/3}]_2O_{4.8}$ transformation of $15K_2O-15Nb_2O_5-70TeO_2$ glass.

$15K_2O-15Nb_2O_5-70TeO_2$ glasses in the temperature range of 50-900°C with different heating rates of 5, 10, 15, 20 and 30 K $minute^{-1}$ are given in Table 3.

The energy of crystallization of the $K[Nb_{1/3}Te_{2/3}]_2O_{4.8}$ phase in $15K_2O-15Nb_2O_5-70TeO_2$ glasses may be calculated from T_x values in Table 3 using the equations of Kissinger or Redhead as follows [24]:

$$\ln(\Phi/T_p^2) = -E/RT_p + \text{const.} \quad (4)$$

where Φ is the heating rate, T_p is the peak temperature, R is the ideal gas constant. As shown in Figure 5, the plot of $\ln(\Phi/T_p^2)$ vs. $(1000/T_p)$ for the $15K_2O-15Nb_2O_5-70TeO_2$ glass showed a straight line. The energy required for the phase transformation from $15K_2O-15Nb_2O_5-70TeO_2$ glass to the $K[Nb_{1/3}Te_{2/3}]_2O_{4.8}$ phase was calculated to be 253.6 kJ/mol from the slope of the straight line. The energy required for crystallization obtained in the $15K_2O-15Nb_2O_5-70TeO_2$ glass is one of the important factors to consider for fabricating the $K[Nb_{1/3}Te_{2/3}]_2O_{4.8}$ phase with a high SHG.

Conclusions

The values of T_g and T_x for the $15K_2O-15Nb_2O_5-70TeO_2$ glass are 375 and 491, respectively. A SHG was clearly observed in $15K_2O-15Nb_2O_5-70TeO_2$ glass-ceramics consisting of a $K[Nb_{1/3}Te_{2/3}]_2O_{4.8}$ phase. The

activation energies for grain growth of the $K[Nb_{1/3}Te_{2/3}]_2O_{4.8}$ phase from the original glasses were determined from the XRD results. The activation energy of grain growth of the $K[Nb_{1/3}Te_{2/3}]_2O_{4.8}$ phase in the $15K_2O-15Nb_2O_5-70TeO_2$ glass was 33.5 kJ/mol. The activation energies of the glass transition and crystallization processes were determined from the shift of T_x with a change of heating rate using Kissinger's or Redhead's equations. The energy for the phase transformation from the $15K_2O-15Nb_2O_5-70TeO_2$ glass to $K[Nb_{1/3}Te_{2/3}]_2O_{4.8}$ phase was determined to be 253.6 kJ/mol.

Acknowledgement

This work has been supported by MOCIE-RTI04-02-01, KBSI grant (No. N26021) and (No. N27074), Korea.

References

1. J.E. Stanworth, *Nature* 169 (1952) 581.
2. P. Balaya and C.S. Sunandana, *J. Non-Cryst. Solids* 162 (1993) 253.
3. A. Abdel-Kader and M. Elkholy, *J. Appl. Phys.* 73 (1993) 71.
4. J. Heo, D. Lam, E. Mendoza, and D. Hensley, *J. Am. Ceram. Soc.* 75 (1992) 277.
5. J.S. Wang, E.M. Vogel, and E. Snitzer, *Opt. Mater.* 3 (1994) 187.
6. R. El-Mallawany, *J. Mater. Res.* 7 (1992) 224.
7. T. Sekiya, N. Mochida, and A. Ohtsuka, *J. Non-Cryst. Solids* 185 (1995) 135.
8. T. Sekiya, N. Mochida, and A. Soejima, *J. Non-Cryst. Solids* 191 (1995) 115.
9. K. Tanaka, K. Kashima, K. Hirao, N. Soga, A. Mito, and H. Nasu, *J. Non-Cryst. Solids* 185 (1995) 123.
10. S.H. Kim and T. Yoko, *J. Am. Ceram. Soc.* 78 (1995) 1061.
11. K. Shioya, T. Komatsu, H.G. Kim, R. Sato, and K. Komatsu, *J. Non-Cryst. Solids* 189 (1995) 16.
12. H.G. Kim, T. Komatsu, K. Shioya, R. Sato, K. Komatsu, K. Tanaka, and K. Hirao, *J. Non-Cryst. Solids* 208 (1996) 303.
13. H.G. Kim, T. Komatsu, R. Sato, and K. Komatsu, *J. Non-Cryst. Solids* 162 (1993) 201.
14. H. Oishi, Y. Benino, and T. Komatsu, *Phys. Chem. Glasses* 40 (1999) 212.
15. T. Watanabe, Y. Benino, K. Ishizaki, and T. Komatsu, *J. Ceram. Soc. Jpn.* 107 (1999) 1140.
16. K. Naito, Y. Benino, T. Fujiwara, and T. Komatsu, *Solid State Comm.* 131 (2004) 289.
17. R.T. Hart, K.M. Ok, P.S. Halasymani, and J.W. Zwanziger, *Appl. Phys. Lett.* 938 (2004) 85.
18. R.T. Hart, M.A. Anspach, B.J. Kraffry, and J.W. Zwanziger, *Chem. Mater.* 12 (2002) 4422.
19. A.A. Bahgat, I.I. Shaltout, and A.M. Elazm, *J. Non-Cryst. Solids* 150 (1992) 179.
20. K. Tanaka, K. Kashima, K. Hirao, N. Soga, A. Mito, and H. Nasu, *Jpn. J. Appl. Phys.* 32 (1993) L843.
21. B.D. Cullity, 2nd Edition, Addison-Wesley Publishing Company, Inc., Reading, MA, 1978.
22. R.L. Coble, *J. Appl. Phys.* 32 (1961) 787.
23. M. Jarcho, C.H. Bolen, and R.H. Doremus, *J. Mater. Sci.* 11 (1976) 2027.
24. H.E. Kissinger, *J. Res. Natl. Bur. Stand. (US)* 57 (1956) 217.